Measurement 131 (2019) 664–670

Contents lists available at ScienceDirect

Measurement

journal homepage: www.elsevier.com/locate/measurement

A heuristics-based method for obtaining road surface type information from mobile lidar for use in network-level infrastructure management

Saurav R. Neupane [a], Nasir G. Gharaibeh [b,*]

[a] Texas A&M University, Zachry Department of Civil Engineering, College Station, TX 77843, United States
[b] Texas A&M University, Zachry Department of Civil Engineering, 3136 TAMU, College Station, TX 77843, United States

ARTICLE INFO

Article history:
Received 15 May 2018
Received in revised form 5 September 2018
Accepted 6 September 2018
Available online 8 September 2018

Keywords:
Lidar
Laser reflected signal intensity
Roadway asset management
Roadway maintenance management

ABSTRACT

Road surface type is a key input to most asset management and maintenance management models and analyses, such as deterioration prediction models, life cycle cost analysis, and need estimates. However, surface type changes in space and time due to the use of varying pavement types and the application of different surface treatments. In recent years, the transportation and municipal industry has begun to use mobile lidar (Light Detection and Ranging) systems to collect roadway condition and inventory data, including surface type. This paper provides a heuristics-based method for detecting road surface type based on statistical analysis of laser reflected signal intensity. The studied surfaces are open graded asphalt, dense graded asphalt, seal coated asphalt, concrete, and roadside vegetation. This method will improve the availability and quality of surface type data, especially for large roadway networks, by automating the process of obtaining this information from mobile lidar measurements.

1. Introduction

To ensure optimal maintenance and rehabilitation of roadway assets over their life cycle, transportation agencies and municipalities use asset management software systems [1]. These software systems analyze roadway condition, inventory, and utilization data to develop optimal multi-year maintenance and rehabilitation (M&R) plans for roadway networks and provide answers to three key questions: What roadway assets should be renewed?; When should these assets be renewed?; and How should they be renewed? Fig. 1 shows the framework in which asset management systems operate.

Pavement surface type is a key input to most asset management models and analyses, such as deterioration prediction models, life cycle cost analysis, and need estimates [2,3]. Information on vegetation areas is used by roadside maintenance systems (e.g., vegetation management). However, surface type changes in space and time due to the use of varying pavement types and the application of different surface treatments (typically used to improve surface characteristics such as friction and smoothness) within the same network. Thus, keeping track of surface type is a major challenge, especially for large roadway networks. For example, the Texas Department of Transportation (TxDOT) maintains approximately 200,000 lane-miles of roads comprised of multiple and changing surface types. In recent years, the transportation infrastructure industry (e.g., municipalities and transportation agencies) has begun to use mobile lidar (Light Detection and Ranging) systems to collect roadway condition and inventory data, including surface type, for use in asset management systems [4,5]. While mobile lidar systems (MLSs) collect large amounts of data rapidly, processing these data to obtain surface type remains expensive and time-consuming, especially for large roadway networks.

The aim of this paper is to improve the use of mobile lidar in transportation asset management by providing a heuristics-based method for automated identification of road surface type from laser intensity measurements obtained from MLSs. It is envisioned that this method will improve the availability and quality of surface type data, especially for large roadway networks.

In the next sections of this paper, we describe the developed method and test it on actual roadway sections. We begin, however, with a review of the literature on lidar technology and surface type identification methods.

2. Background

Generally, measurements collected by a lidar system include incidence angle, slant distance, and laser intensity. In this paper, we use reflected laser signal intensity, a measure of return signal strength, to identify surface type for use in pavement and roadside

* Corresponding Author.
E-mail address: ngharaibeh@civil.tamu.edu (N.G. Gharaibeh).

https://doi.org/10.1016/j.measurement.2018.09.015
0263-2241/

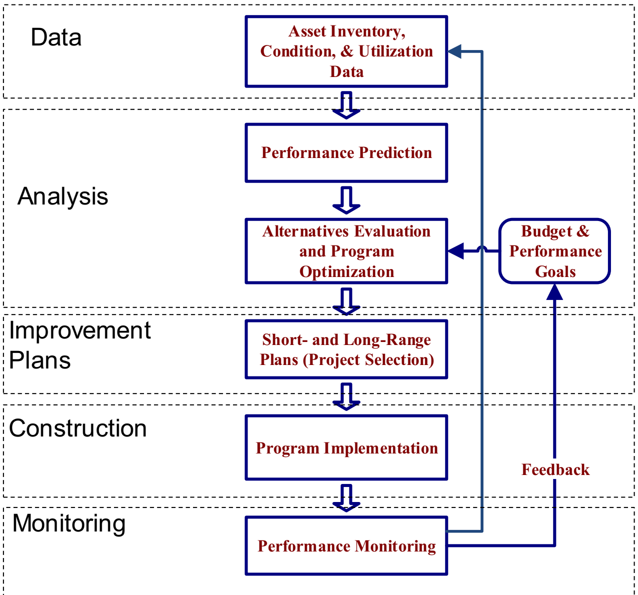

Fig. 1. Infrastructure asset management framework.

asset management systems. Laser intensity has been used in a variety of applications, such as classification of natural and built urban cover surfaces, identification of snow covered areas, lava flow and aging, rock properties, coastal land cover, and flood modeling [6].

Laser intensity varies by surface reflectance and roughness, and other confounding variables, such as range, angle of incidence, transmittal power, atmospheric transmittance, and scanning environment. Kashani et al. [6] grouped these factors into four categories: a) target surface characteristics (i.e., reflectance and roughness), b) data acquisition geometry, c) instrument effects, and d) environmental effects. Lidar systems normally implement intensity processing techniques to minimize the effect of these confounding variables and produce intensity values that are more closely related to the true surface characteristics. These processes have been classified as intensity correction, intensity normalization, and rigorous radiometric correction and calibration [6]. Significant advances have been made in the development of algorithms for identifying pavement surface characteristics and condition from digital images [7–10] and hyperspectral imagery [11–13]. However, despite the penetration of mobile lidar into the transportation and municipal industry, methods for identifying road surface type from mobile lidar measurements are still lacking. One of the early efforts in automated identification of roadway characteristics from aerial lidar data is described in [14]. In this paper, we focuses on mobile lidar and aim to improve the use of this technology in transportation asset management by providing a heuristics-based method for automated identification of road surface type.

3. Data collection and analysis

A pulse-scanning MLS unit was used to measure reflected signal intensity in terms of Received Signal Strength Indicator (RSSI) for 61.3 km (38.1 miles) of road located in different parts of Texas, USA (Table 1). The data were collected in dry weather conditions (i.e., no wet surfaces were included) in December-January. RSSI is a dimensionless 8-bit measure of reflected signal intensity, ranging from zero to 255.

Intensity is affected by the reflectivity of the pavement surface struck by the laser pulse. The pavement surfaces of these roadway sections are concrete, dense graded asphalt, open graded asphalt, and seal coated asphalt. The roadway network in Texas is composed predominantly of these pavement types. While gravel roads are common in many parts of the world (e.g., low-volume roads), seal coated asphalt is often used in Texas in lieu of bare gravel. Seal coating consists of spraying one or more layers of bituminous binder; each layer is followed by spreading a layer of aggregates [15]. Sections 5–7 include roadside vegetation areas.

The MLS includes a single planar SICK LMS-5XX series laser scanner, a forward-facing video camera, a global positioning system (GPS) unit, and an inertial measurement unit (IMU) (Fig. 2). The wavelength of light emitted by the laser scanner is 905 nm. The IMU was used to improve the accuracy of the lidar point cloud collected at high traffic speeds [16]. For pavement surfaces, intensity was measured within approximately one meter on each side of the MLS centerline (in the transverse direction). For roadside, intensity was measured between the edge of pavement and approximately four meters into the roadside (i.e., approximately 6 m from the MLS centerline). These distances were used to minimize the need for interpolation between measurements, obtain sufficient point density, and lessen intensity attenuation. As the distance between the MLS and the target increases, the spacing between the measurement points becomes wider; which decreases point density and may necessitate interpolation between measurements. For example, for a 1 m $\times$ 1 m grid along the right roadside of a rural roadway with shoulder, no interpolation is required between the edge of pavement and approximately 4.6 m [17].

Road surface characteristics such as texture, granulation size, color, and porosity affect laser intensity [18]; resulting in different RSSI values. The developed method uses RSSI values to identify surface type. To uncover possible patterns in intensity measurements, laser intensity data for the studied roadway sections were plotted in frequency distributions (Fig. 3).

As can be observed from Fig. 3, the intensity distributions for open graded and dense graded asphalt are very similar, possibly due to similarity in surface color and texture. Compared to con-

Table 1
Data collection sites (Central and East Texas).

Section no.	Road name	Length, km	Pavement area, m^2	Pavement surface	Filtered no. of intensity measurements
1	George Bush Drive[(1)]	7.2	14,400	Concrete	1,091,721
2	Penberthy Road[(1)]	4.3	8,600	Concrete	643,068
3	University Drive[(1)]	7.1	14,200	Dense Graded Asphalt	868,329
4	Texas Highway 6[(1)]	11.2	22,400	Open Graded Asphalt	1,702,827
5	Farm-to-Market (FM)95[(1)]	18.0	36,000	Seal Coated Asphalt	1,483,840
6	FM320[(2)]	11.7	23,400	Seal Coated Asphalt	1,388,874
7	FM2661[(2)]	0.3	600	Seal Coated Asphalt	47,483

[(1)] Central Texas.
[(2)] East Texas.

Fig. 2. MLS used in data collection, consisting of SICK LMS-5XX laser scanner, GPS Unit, IMU, forward looking video camera, and data storage and processing systems.

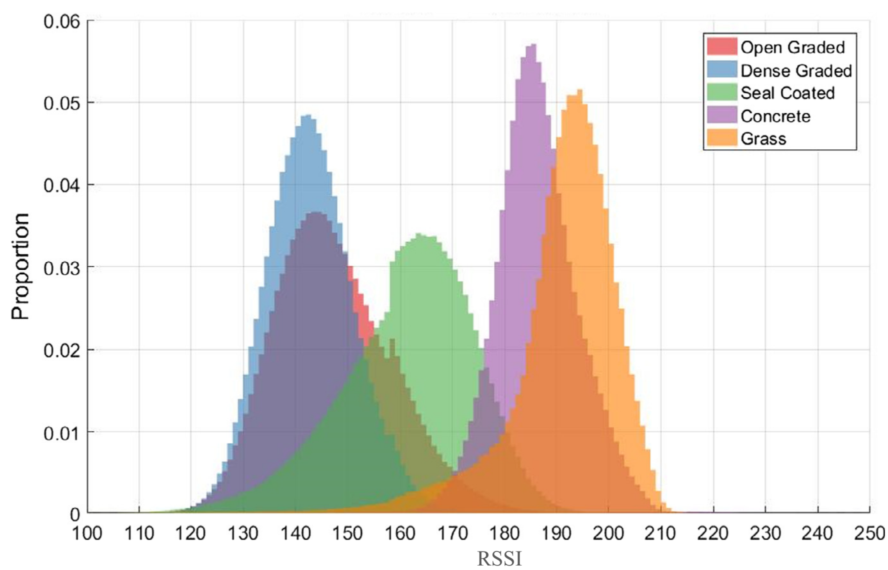

Fig. 3. Frequency distributions of laser reflected signal intensity measurements for road surfaces considered in this study.

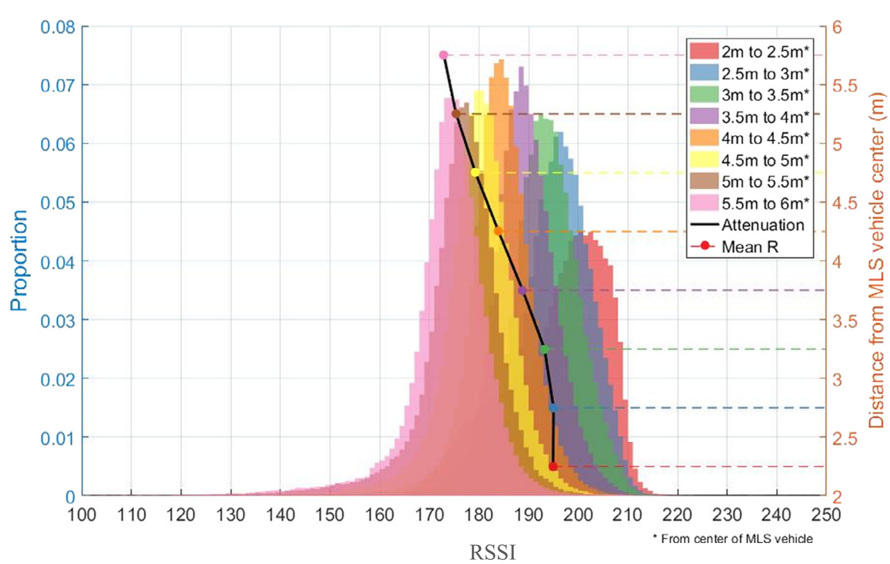

Fig. 4. Attenuation of laser reflected signal intensity for roadside vegetation on FM95.

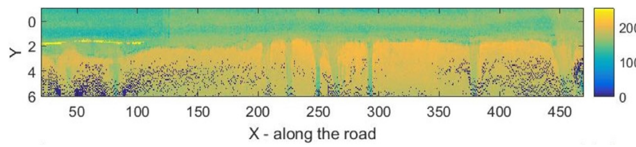

a) Laser reflected signal intensity before correction

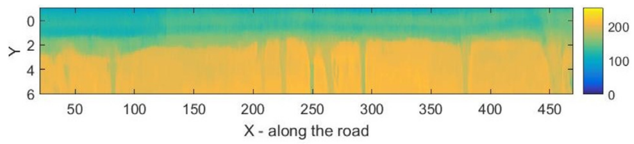

b) Laser reflected signal intensity after correction

Fig. 5. Plan view of a road section color-coded based on reflected signal intensity (X and Y are distance in meters; legend is RSSI scale).

crete surface, asphalt surfaces exhibit higher variability in laser intensity, possibly due to the higher variability in color and texture. Generally, the studied asphalt pavement sections have varying age (which leads to changes in color due to varying levels of binder oxidation) and include more patching (which leads to changes in texture).

Identifying vegetation from intensity data is more challenging than identifying pavement surface type because the roadside is highly irregular in terms of composition, texture, and color. Also, the roadside extends in the transverse direction further away from the MLS centerline. As shown in Fig. 4, the intensity distributions for roadside areas attenuate as the lidar measurements move away from the MLS center in the transverse direction. Therefore, intensity data from the roadside (assuming that roadside begins 2.25 m from the MLS center) were corrected for impurities (e.g., gravel areas) and attenuation using the following regression equation:

$$\Delta_S = 8.03d - 17.82 \tag{1}$$

where Δ_S is the difference between mean intensity at any given transverse horizontal distance, d, from the MLS center and the intensity at 2.25 m from the MLS in the transverse direction (i.e., distance at which roadside vegetation normally begins). A quadratic attenuation equation ($\Delta_S = -0.06d^2 + 8.53d - 18.74$) was developed and tested during the initial development phase. However, no significant effect on the overall method's performance was observed, and thus the linear function was adopted for simplicity. Fig. 5 depicts laser intensity on the plan view of a sample road section before and after the intensity from the roadside surface was corrected using Eq. (1).

The processed data were used to establish reference distributions for each surface type. Fig. 6 depicts the reference intensity distributions for the four pavement surfaces and the roadside vegetation considered in this study. The mean and standard deviation for these reference distributions are presented in Table 2.

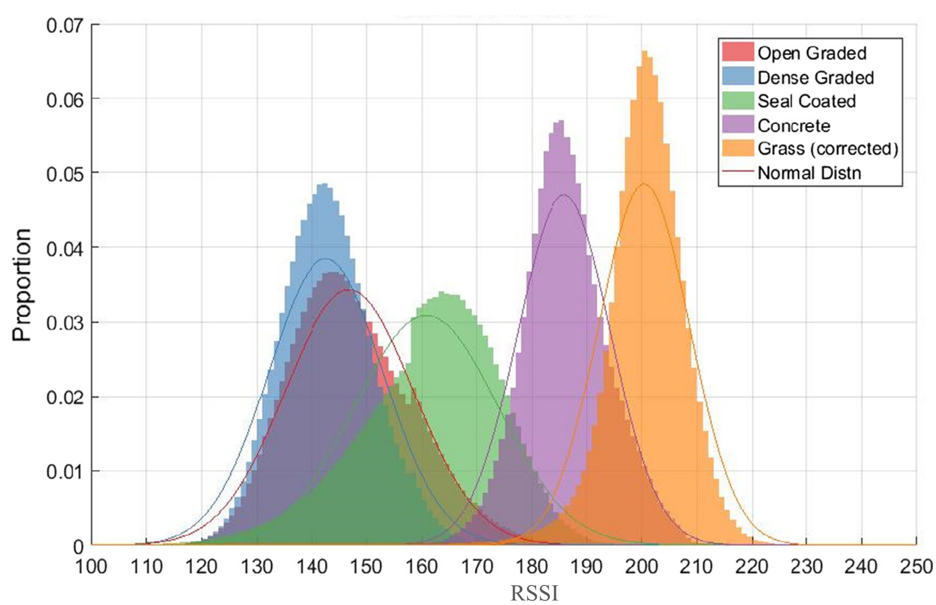

Fig. 6. Reference reflected signal intensity distributions for the studied surfaces.

Table 2
RSSI mean and standard deviation for studied surfaces.

Parameter	Open Graded Asphalt	Dense Graded Asphalt	Seal Coated Asphalt	Concrete	Roadside Vegetation*
Mean	146.8	142.6	160.9	185.9	200.5
Standard Deviation	11.6	10.4	12.9	8.5	8.2

* Attenuated and corrected.

4. Surface type identification method

During the initial development phase, the Support Vector Machine and the K-Nearest Neighbor classification methods were considered. However, that approach was not pursued in favor of a heuristics-based method to facilitate adoption by the transportation and municipal industry, without compromising rigor. Also, the autocorrelation/power spectrum was considered during the initial development phase. While seal coated sections exhibited multiple peaks for selected nonequispaced fast Fourier transforms, no discernable pattern was found. There was a lack of any significant spatial periodicity. Thus, intensity spectral distribution was excluded from further consideration. Due to the lack of periodicity and the lack of observable patterns in the variance and kurtosis, the mean and skewness of RSSI (a measure of reflected signal intensity) were deemed key for identifying road surface type. The developed algorithm begins by identifying surface type based on skewness and closeness to mean of reference distributions (Fig. 7). RSSI skewness and closeness to reference mean are computed as follows:

$$S_R = \frac{E(R-\mu_R)^3}{\sigma_R^3} \tag{2}$$

where S_R = Pearson's moment coefficient of skewness of RSSI for subject section, μ_R = mean of RSSI for subject section, σ_R = standard deviation of RSSI for subject section, and E(t) represents the expected value of the quantity *t*.

$$\Delta_R = |\mu_R - \mu_{R^*}| \tag{3}$$

where Δ_R = Closeness of RSSI to reference mean, μ_R = Mean RSSI for subject section, μ_{R^*} = Mean RSSI for reference distribution.

When the mean RSSI for the subject section (i.e., section for which surface type is being identified) is relatively equidistant from the mean values of seal coated and concrete reference distributions, or mean values of seal coated and dense graded reference distributions, skewness is used to distinguish seal coated surface from other surface types. Otherwise, the type corresponding to the closest reference mean is identified as surface type for the subject section. The threshold values and constants used in this algorithm were determined using an iterative process to maximize the agreement between the detected surface type and the true surface type.

For network-level applications, additional steps were added to the algorithm to account for consistency in detected surface type for adjacent pavement sections (Fig. 8). If adjacent sections have no predominant surface type, no change is made to the surface type identified based on intensity skewness and closeness to reference mean.

For identifying roadside vegetation areas, first, the algorithm identifies the pavement surface as either concrete or asphalt, then it distinguishes between vegetation and asphalt surfaces or between vegetation and concrete surfaces using the same process described in Fig. 7.

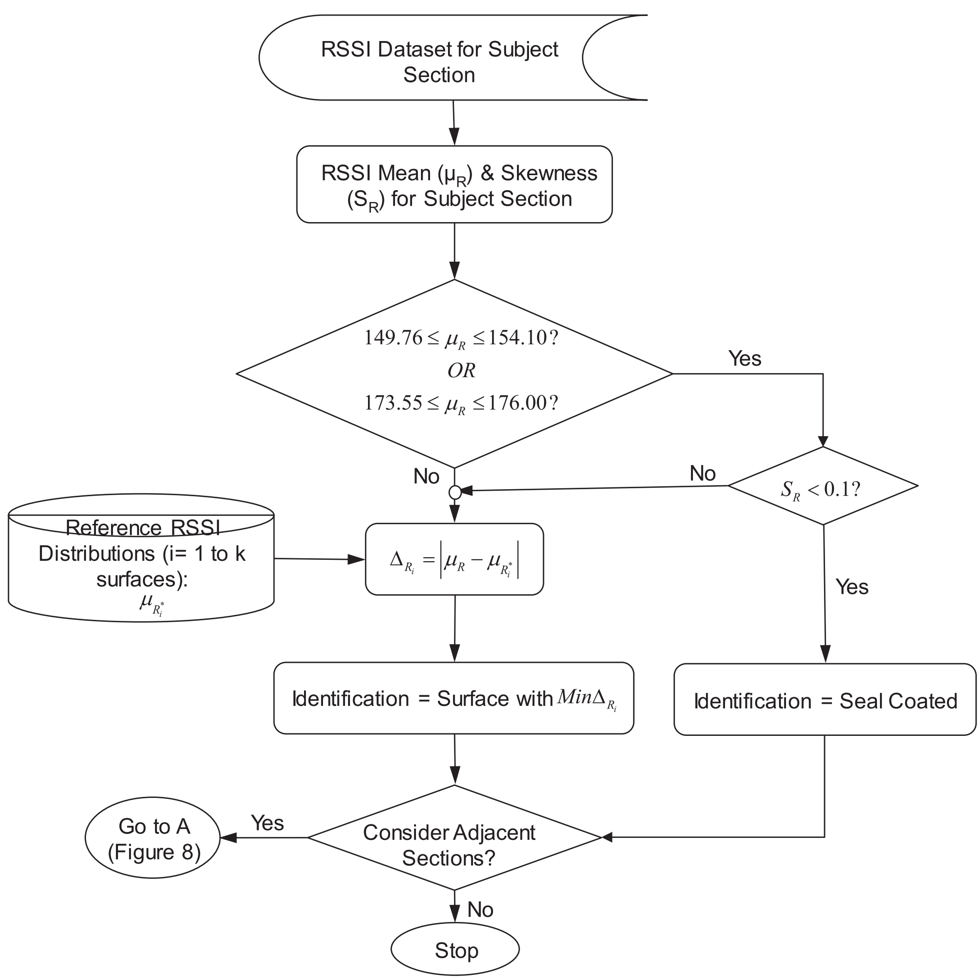

Fig. 7. Detection of surface type based on RSSI skewness and closeness to reference mean.

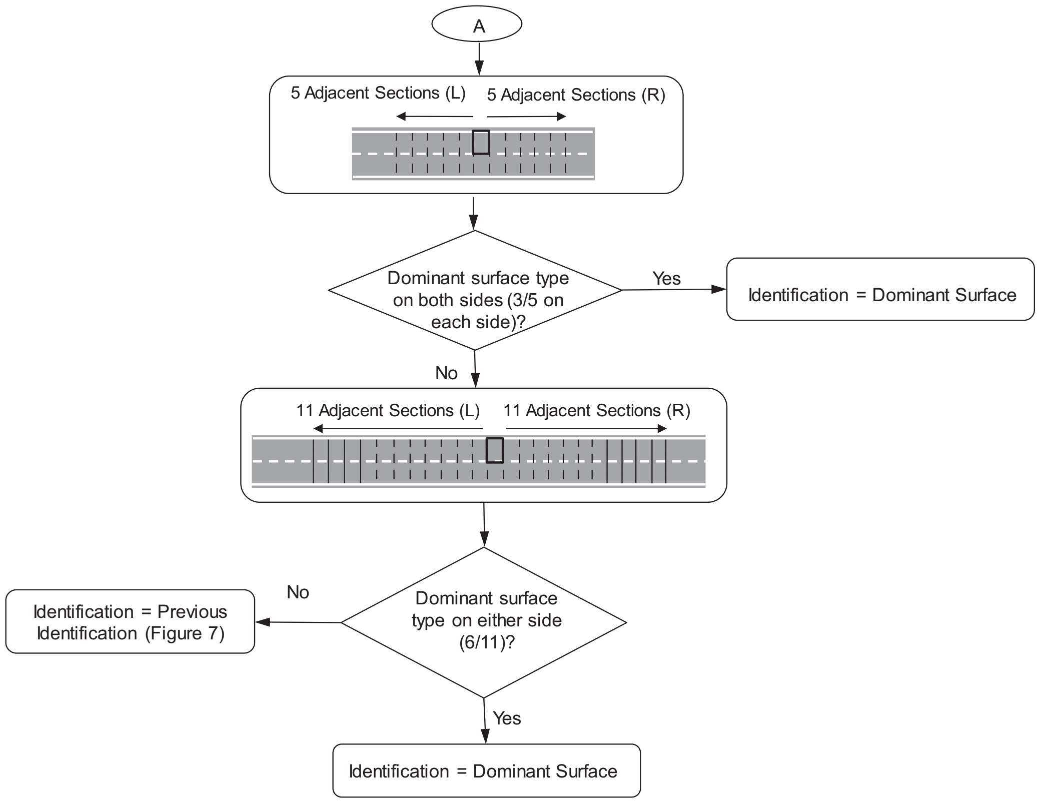

Fig. 8. Adjustment of pavement surface type based on adjacent sections.

5. Validation and limitations of the developed method

The developed method was tested using randomly-selected roadway sections from the study dataset. The length of the test sections was varied from approximately 20 m (66 feet) to 161 m (528 feet), resulting in thousands of test sections. In each run, the developed method analyzed the intensity data from the randomly-selected test section in two sequential stages: 1) identified pavement surface type, and 2) delineated the area of roadside vegetation, given the pavement type identified in stage 1. The outcome of stage 1 is one of four possible pavement types (concrete, dense graded asphalt, open graded asphalt, seal coated asphalt), whereas the outcome of stage 2 is one of two possible surface types (vegetation or the pavement type identified in stage 1). Thus, the evaluation of model accuracy in identifying roadside vegetation areas was done for concrete roads and asphalt roads separately.

In each test, a portion of the intensity data for each surface type was used as the reference data and the remaining portion was used as subject data. To remove biases in data selection, the reference data and subject data were always selected at random from the overall data sets. Accuracy is calculated as follows:

$$Accuracy = \frac{TP + TN}{N} * 100 \tag{4}$$

where TP = True positives (number of times surface correctly identified as subject surface); TN = True negative (number of times surface correctly identified as non-subject surface); N = Total number of subject sections in the test data set. When the subject section is of a single surface, TN is zero.

Table 3 shows the algorithm's accuracy in identifying pavement surface type through classification into four possible outcomes (concrete, dense graded asphalt, open graded asphalt, or seal coated asphalt) for 80.5 m (0.05-mile) subject pavement sections. When the algorithm is based solely on intensity measurements (i.e., disregarding adjacent sections), the algorithm's accuracy was at least 88% for concrete, seal coated asphalt, and open graded asphalt surfaces; but markedly lower (63.3%) for dense graded asphalt pavement. The dense graded results can be explained by the similarity in the intensity distributions for dense graded and open graded surfaces, making it difficult to distinguish between these two surfaces. When adjacent pavements are considered (in combination with intensity skewness and closeness to reference mean), however, the algorithm's accuracy increases for all cases; most noticeably for dense graded surfaces where accuracy increased to 73.3%. Similar accuracy was achieved when the size of the reference data sets and size of subject sections were varied.

To test the algorithm's accuracy in detecting roadside vegetation, one thousand random samples were extracted from the

Table 3
Accuracy of the developed method in identifying pavement surface type for 80.5 m (0.05-mile) subject sections.

Surface type	Algorithm based on closeness to RSSI reference mean and skewness	Algorithm based on closeness to rssi mean, skewness, & consistency among adjacent sections
Concrete	95.39%	100%
Dense Graded Asphalt	63.33%	73.33%
Open Graded Asphalt	88.44%	89.33%
Seal Coated Asphalt	92.58%	97.42%

Table 4
Results of identification of roadside vegetation areas (Concrete roads).

Actual surface	Percent intensity points identified As	
	Vegetation	Concrete
Vegetation	90.3	9.7
Concrete	16.3	83.7

Table 5
Results of Identification of Roadside Vegetation Areas (Asphalt Roads).

Actual surface	Percent intensity points identified As	
	Vegetation	Asphalt
Vegetation	98.7	1.3
Asphalt	1.0	99.0

studied sections after grouping them into asphalt roads – open graded, dense graded, and seal coated combined – and concrete roads. For concrete roads (Table 4), 90.3% of the vegetation samples were correctly identified and 9.7% were misidentified as concrete. For asphalt roads (Table 5), 98.7% of the vegetation samples were correctly identified and 1.3% were misidentified as asphalt. Thus, the developed algorithm is more accurate when identifying roadside vegetation areas on asphalt roads than on concrete roads.

The method described in this paper has limitations that could be addressed in future work, as follows.

- The data used in this study were collected on dry paved roads in east central Texas in December-January. Future work could test and calibrate the developed method for a wider range of weather conditions (e.g., wet surfaces), seasons (e.g., different vegetation condition), and surface types (e.g., gravel roads). Wet surfaces, in particular, are a major issue because many current laser scanners cannot capture them.
- The method could be extended to distinguish between pavement and gravel shoulders.
- Generally, the intensity data from pavements in good condition were observed to have less kurtosis compared to cracked pavements (sealed or unsealed cracks). Future work could consider distinguishing between pavement in good condition and pavement in poor condition.
- Attenuation correction could be expanded to consider angle of incidence, instrument parameters, and surface/material condition.

6. Summary and conclusions

This paper describes the development and validation of a heuristics-based method for automated identification of road surface types from laser reflected signal intensity measurements obtained from a mobile lidar unit. The algorithm was developed and tested using data collected from 61.3 km (38.1 miles) of roads in Texas, USA, representing four pavement surface types (open graded asphalt, dense graded asphalt, seal coated asphalt, and concrete) and roadside vegetation. The method identifies surface type based on the intensity skewness and closeness to the mean of reference distributions. For network-level applications, the method takes into consideration the detected surface type of adjacent pavement sections. If adjacent sections have no predominant surface type, no change is made to the surface type identified based on intensity skewness and closeness the mean of reference a distributions. When the method is based solely on intensity measurements (i.e., disregarding adjacent sections), its accuracy is at least 88%; except for dense graded pavement where accuracy drops to 63.3%. These results can be explained by the similarity in the laser intensity distributions for dense graded and open graded asphalt surfaces, making it difficult to distinguish between these two surfaces. When adjacent pavements are considered, however, the algorithm's accuracy increases for all cases; most noticeably for dense graded asphalt surfaces where accuracy increases from 63.3% to 73.3%. Roadside vegetation areas were identified correctly 98.7% and 90.3% of the time for asphalt and concrete roads, respectively. Thus, the developed method is more accurate when identifying roadside vegetation areas on asphalt roads, compared to concrete roads.

References

[1] American Association of State Highway and Transportation Officials (AASHTO). Transportation Asset Management Guide. RP-TAMG-1, Washington, DC, 2002.
[2] J.R. Menendez, S. Zabihi Siabil, P. Narciso, N.G. Gharaibeh, Prioritizing infrastructure maintenance and rehabilitation activities under various budgetary scenarios: evaluation of worst-first and benefit-cost analysis approaches, Transp. Res. Rec.: J. Transp. Res. Board 2361 (2013) 56–62.
[3] O. Swei, J. Gregory, R. Kirchain, Probabilistic characterization of uncertain inputs in the life-cycle cost analysis of pavements, Transp. Res. Rec, J Transp. Res. Board. 2366 (2013) 71–77.
[4] K. Williams, M.J. Olsen, G.V. Roe, C. Glennie, Synthesis of transportation applications of mobile LIDAR, Remote Sens. 5 (9) (2013) 4652–4692.
[5] M. Varela-González, H. González-Jorge, B. Riveiro, P. Arias, Automatic filtering of vehicles from mobile LiDAR datasets, Measurement 53 (2014) 215–223.
[6] A.G. Kashani, M.J. Olsen, C.E. Parrish, N. Wilson, A Review of LiDAR radiometric processing: from ad hoc intensity correction to rigorous radiometric calibration, Sensors (Basel, Switzerland) 15 (11) (2015) 28099–28128.
[7] D.M. Tsai, C.T. Lin, Fast normalized cross correlation for defect detection, Pattern Recognit. Lett. 24 (15) (2003) 2625–2631.
[8] K.C.P. Wang, O. Smadi, Automated imaging technologies for pavement distress surveys, Transp. Res. (2011), Circular E-C156.
[9] Uslu, B., Golparvar-Fard, M., de la Garza, J.M., 2011. Image-Based 3D Reconstruction and Recognition for Enhanced Highway Condition Assessment. In: Zhu, Y., Issa, R.R., Conf. Proc., International Workshop on Computing in Civil Engineering, June 19–22, 2011 Miami, Florida, pp. 67–76.
[10] S. Wang, S. Qiu, W. Wang, D. Xiao, K.C.P. Wang, Cracking classification using minimum rectangular cover-based support vector machine, J. Comput. Civil Eng. 31 (5) (2017) 04017027, https://doi.org/10.1061/(ASCE)CP.1943-5487.0000672.
[11] M. Mohammadi, Road classification and condition determination using hyperspectral imagery, Int. Arch. Photogramm. Remote Sens. 39 (2012) 141–146.
[12] M. Herold, D. Roberts, Spectral characteristics of asphalt road aging and deterioration: implications for remote-sensing applications, Appl. Opt. 44 (20) (2005) 4327–4334.
[13] P. Jonsson, J. Casselgren, B. Thornberg, Road surface status classification using spectral analysis of NIR camera images, IEEE Sens. J. 15 (3) (2015) 1641–1656.
[14] S.J.C. Beck, M.J. Olsen, J. Sessions, M.G. Wing, Automated extraction of forest road network geometry from aerial LiDAR, Eur. J. For. Eng. 1 (1) (2015) 21–33.
[15] S. Labi, K.C. Sinha, Effectiveness of highway pavement seal coating treatments, J. Transp. Eng. 130 (1) (2004) 14–23, https://doi.org/10.1061/(ASCE)0733-947X(2004) 130:1(14).
[16] H.J. Yoo, F. Goulette, J. Senpauroca, G. Lepere, Analysis and improvement of laser terrestrial mobile mapping systems configurations, Int. Arch. Photogramm. Remote Sens. 38 (PART 5) (2010) 633–638.
[17] C.F. Gurganus, N.G. Gharaibeh, T. Scullion, Case study on the use of mobile lidar to produce a preliminary drainage design, Transp. Res.: J. Transp. Res. Board 2655 (2017) 82–90, https://doi.org/10.3141/2655-11.
[18] W.H. Johnson, A.M. Johnson, Operational considerations for terrestrial laser scanner use in highway construction applications, J. Surv. Eng. 138 (4) (2012) 214–222, https://doi.org/10.1061/(ASCE)SU.1943-5428.0000084.